IOPscience iopscience.iop.org

Home Search Collections Journals About Contact us My IOPscience

The equivalent ellipsoid of a magnetized body

This content has been downloaded from IOPscience. Please scroll down to see the full text.

View the table of contents for this issue, or go to the journal homepage for more

Download details:

IP Address: 129.132.209.201
This content was downloaded on 22/01/2015 at 12:46

Please note that terms and conditions apply.

INSTITUTE OF PHYSICS PUBLISHING JOURNAL OF PHYSICS D: APPLIED PHYSICS

J. Phys. D: Appl. Phys. **39** (2006) 891–899 doi:10.1088/0022-3727/39/5/001

The equivalent ellipsoid of a magnetized body

M Beleggia[1], **M De Graef**[2] **and Y T Millev**[3]

[1] Brookhaven National Laboratory, Building 480, Upton, NY 11973, USA
[2] Department of Materials Science and Engineering, Carnegie Mellon University, Pittsburgh, PA 15213-3890, USA
[3] American Physical Society, 1 Research Road, Ridge, NY 11961, USA

E-mail: beleggia@bnl.gov

Received 10 August 2005, in final form 13 December 2005
Published 17 February 2006
Online at stacks.iop.org/JPhysD/39/891

Abstract
The equivalent ellipsoid for magnetized bodies of arbitrary shape can be determined by imposing the equality between the demagnetization factors of the two shapes of equal volume. It is shown that the 'commonsense' criterion for mapping two different shapes by imposing the equality of the demagnetization factors for equal aspect ratios often results in large errors. We propose a general method for the rigorous determination of the equivalent ellipsoid. The cases of the exact equivalent ellipsoids for discs, cylinders with elliptical cross section and prisms are worked out and discussed.

1. Introduction

There is a general theorem in micromagnetics according to which, under rather relaxed conditions, a body of arbitrary shape is equivalent to an ellipsoid, both of them uniformly magnetized to saturation and of equal volume [1–3]. The concept of the *equivalent ellipsoid* is intuitively very appealing, but it is not straightforward to find the correct shape parameters of an ellipsoid in order to establish this equivalence. The expectation that some symmetrical ferromagnetic bodies would closely resemble an actual ellipsoid may, in fact, be very misleading.

Consider, for instance, the right circular cylinder which, like an ellipsoid of revolution, exhibits axial symmetry. The shape of such a cylinder is determined solely by the ratio of diameter to thickness, known as the aperture of the cylinder. The shape of an ellipsoid of revolution (spheroid) is similarly specified by just the ratio of its axes. It is only fair that in each separate treatment of a cylinder or a spheroid the single shape-characterizing parameter has been called the aspect ratio. It has not been so fair, but has still been seen as intuitively appealing, that identical aspect ratios for a cylinder and for a spheroid were taken to imply identical demagnetizing factors for the corresponding distinct shapes. The appeal of this substitution of one shape (ellipsoid of revolution) for the other (cylinder) seems to have been two-fold. First, until recently [4–6], the demagnetizing factors for the cylinder have only been given in terms of elliptic integrals [7–9] or numerically [10], while the counterpart expressions for the spheroid have been known for quite a while in terms of elementary functions [11, 12]. Second, the admitted error in the demagnetization factor due to this swap of shapes has been thought to be small. Thus, the 'commonsense' trade-off has been rooted in the simplicity of the considered expressions, supplemented by the expectation of a small quantitative error. That the error can actually be quite significant has been noticed in the particular context of spin-reorientation transitions in very thin platelets (discs) [13]; it is also considerable in the other extreme of long cylindrical rods (see below).

The other instance of a nonellipsoidal shape of much practical interest is the square rectangular prism [14]. The analytical expressions are in terms of elementary functions of a single shape parameter even though the rotational symmetry now is only discrete unlike the continuous rotational symmetry of either the spheroid or the cylinder. So once again the self-suggesting correspondence, based on the relevance of a single shape parameter (aspect ratio), has been widely implemented under the trade-off conditions, just described in the previous paragraph. A particular observation of the inadequacy of the commonsense assumption 'equal aspect ratios bring about equal demagnetization factors' has been provided by Aharoni [15], where it is explicitly stated that the theory of a (square) prism with an aspect ratio of 11 should be compared with that of a prolate spheroid with an aspect ratio of about 6.

 © 2006 IOP Publishing Ltd Printed in the UK

As argued convincingly by Chen *et al* [16], where demagnetization factors for prisms, ellipsoids and cylinders (on this shape, also see [17]) were analysed and presented in close connection, the determination of demagnetization factors for different shapes is on the one hand a 'classical topic of magnetism', i.e. a fundamental problem which, even today, presents challenges and open issues; on the other hand, their knowledge stimulated a great deal of experimental investigation (see e.g. references within [16]), with renewed emphasis after the advent of nanoscience, a realm where magnetic clusters, particles and structures may be found spontaneously in single-domain quasi-uniform states. The energetics of such systems may be fully understood only with the availability of correct demagnetization factors, and if the equivalence between a shape of interest and a suitable ellipsoid, for which their knowledge is widely spread, is established then the extraction of physical information may be safer from possible misinterpretations.

It is the objective of this paper to exactly quantify the magnetostatic equivalence of bodies of different shapes to a corresponding uniformly magnetized ellipsoid and to elucidate the important aspects of this equivalence. The analysis goes far beyond the two simplest nonellipsoidal shapes (cylinder and square prism). It generalizes substantially a recent method for the solution of the cylinder–spheroid equivalence [18] by making full use of a very far-reaching Fourier-space approach to the analytical calculation of the demagnetization factors of arbitrary shapes [5, 6, 19]. The advance reported here focuses on the rigorous and conclusive description of the equivalence to a suitable ellipsoid of magnetized bodies, whose shape is described by two dimensionless parameters. In particular, right cylinders with elliptical cross section and general rectangular parallelepipeds are examined. In each of these classes of shape, the equivalent ellipsoid is a general triaxial one with two independent aspect ratios. The problem is then by one continuous degree of freedom more complicated than those for the circular cylinder and the square prism and, magnetostatically, one has to deal with two independent demagnetization factors, each of them a function of two independent aspect parameters.

The scheme of exposition given below will be followed. First, the concept of the equivalent ellipsoid is discussed in sufficient detail and the relevant facts about the analytical expressions for the demagnetization factors of the general ellipsoid are brought in. Next, the equivalent ellipsoid for the right circular cylinder ('plain cylinder') is determined. Then, the cases of the right cylinder with an elliptical cross section and of the general rectangular prism are examined in succession. Obviously, one could have derived the particular case of the circular cylinder as a limiting case from the general results for the elliptical cylinder. However, an understanding of the plain cylinder will give the reader a grip on the extension of the method to the more involved cases. The same observation holds for the square prism being a particular case of the general rectangular prism, but here we do not discuss separately the procedure as it follows the one for the plain cylinder. A summary of the scope and some possible extensions of this work is provided at the end.

2. General considerations

Let us first briefly recall the concept of the equivalent ellipsoid. For uniformly magnetized bodies where $\boldsymbol{M}(\boldsymbol{r}) = M_0\boldsymbol{m}$, the magnetostatic energy can be written as a quadratic form [2, 10, 20, 21]:

$$\begin{aligned} E_\mathrm{m} &= -\frac{\mu_0}{2}\int_{\mathcal{D}} \boldsymbol{M}(\boldsymbol{r})\cdot\boldsymbol{H}(\boldsymbol{r})\,\mathrm{d}^3\boldsymbol{r} \\ &= -\frac{\mu_0 M_0}{2}\sum_{i=1}^{3}\int_{\mathcal{D}} m_i H_i(\boldsymbol{r})\,\mathrm{d}^3\boldsymbol{r} \\ &= K_\mathrm{d}\sum_{i,j=1}^{3}\int_{\mathcal{D}} m_i N^{ij}(\boldsymbol{r}) m_j\,\mathrm{d}^3\boldsymbol{r} \\ &= K_\mathrm{d} V\sum_{i,j=1}^{3} m_i \langle N\rangle^{ij} m_j \\ &= K_\mathrm{d} V (N_x m_x^2 + N_y m_y^2 + N_z m_z^2), \end{aligned} \tag{1}$$

where $\mathcal{D}$ stands for the domain of space, bounded by the particle surface, $K_\mathrm{d} = \mu_0 M_0^2/2$ is the magnetostatic energy density, V is the particle volume, $N^{ij}(\boldsymbol{r})$ is the local position-dependent demagnetization tensor connecting the $\boldsymbol{M}$ and $\boldsymbol{H}$ fields and $\langle N\rangle^{ij}$ is the magnetometric (volume averaged) demagnetization tensor. The diagonal elements of the tensor $\langle N\rangle^{ij}$ are the demagnetization factors, N_i, of the body. The three demagnetization factors of a shape are not independent as the trace of the tensor is unity on general magnetostatic grounds [2, 20–22]. Hence, $N_x + N_y + N_z = 1$. For shapes with rotational symmetry about the z-axis, only one factor (say, N_z) remains independent, as $N_x = N_y = \frac{1}{2}(1 - N_z)$.

From (1) it is evident that two bodies of equal volume, equal saturation magnetization and equal demagnetization factors possess the same magnetostatic energy. Since the demagnetization factors for a generic triaxial ellipsoid were known [11, 12], while the knowledge of the demagnetization factors for other shapes was very difficult to obtain, it became customary to treat any shape as an ellipsoid, assuming implicitly that some self-suggesting criterion for choosing its semiaxes was reasonable. Usually, equality of the corresponding aspect ratios under the condition of equal volumes has been deemed sufficiently accurate without actually attempting to control the error analytically. It will soon be seen that even for a shape as simple as that of the disc such an intuitive criterion introduces substantial errors in the magnetostatic energy. The demagnetization factors for the general ellipsoid belong to the body of well-established results of magnetostatics. They are reproduced here for the convenience of making this work self-contained. It is worth noting that the depolarization factors of electrostatics are identical to the demagnetization ones and are at least as important [23]. Let us denote by (a, b, c) the ellipsoid semiaxes and let the two independent aspect ratios be $\tau_a = c/a$ and $\tau_b = c/b$. Then,

$$N_z(\tau_a, \tau_b) = \frac{1}{\tau_a\tau_b}\frac{F(k,m) - E(k,m)}{m\sin^3 k}, \tag{2}$$

with

$$k = \arcsin\sqrt{1-\tau_a^{-2}} \qquad \text{and} \qquad m = \frac{1-\tau_b^{-2}}{1-\tau_a^{-2}}, \tag{3}$$

where $E(k, m)$ and $F(k, m)$ are incomplete elliptic integrals [24].

Although in the literature the other two demagnetization factors N_x and N_y are always given along with N_z, we choose to exploit a symmetry of the problem that seems to have remained unnoticed so far. Namely, to evaluate the N_x demagnetization factor one can virtually rotate the ellipsoid along the y-axis and consider that N_x of the original ellipsoid is N_z of the rotated one with the corresponding aspect ratios. This procedure results in the following very useful and compact relations, which allow us to totally bypass the need to introduce explicitly any factors other than N_z:

$$N_x(\tau_a, \tau_b) = N_z\left(\frac{1}{\tau_a}, \frac{\tau_b}{\tau_a}\right), \tag{4}$$

and similarly for the N_y factor:

$$N_y(\tau_a, \tau_b) = N_z\left(\frac{\tau_a}{\tau_b}, \frac{1}{\tau_b}\right). \tag{5}$$

Note that this procedure is allowed only when an expression for N_z is available, which remains well defined for arbitrary values of the aspect ratios in the range $(0 \leqslant \tau_{a,b} \leqslant +\infty)$. As it stands above, if N_z in (2) was defined only for, say, $0 < \tau_a < 1$, in order to make sure that the parameter k defined in (3) remains real-valued then N_x would be ill-defined because it requires the evaluation of the same function N_z outside its domain of validity. However, it can be verified working in the complex plane that (2) remains valid for arbitrary values of the aspect ratio, although some of the arguments of the functions involved are complex numbers [12]. Therefore, no further knowledge beyond $N_z(\tau_a, \tau_b)$ is actually needed. For ellipsoids with rotational symmetry (oblate or prolate spheroids), where $\tau_a = \tau_b \equiv \tau_e$, one can simplify the expression for N_z as follows:

$$N_z(\tau_e) = \frac{1}{1-\tau_e^2}\left[1 - \frac{\tau_e \arccos(\tau_e)}{\sqrt{1-\tau_e^2}}\right], \tag{6}$$

while the other two factors are, trivially, $N_x = N_y = \frac{1}{2}(1-N_z)$. As a final verification, it is easy to show that when $\tau_e = 1$ (sphere), $N_x = N_y = N_z = 1/3$.

3. The equivalent ellipsoid for cylinders

A general cylinder of thickness (height) t and radius R with aspect ratio $\tau = t/2R$ is characterized by the following demagnetization factor along the cylinder axis [4, 6]:

$$\begin{aligned} N_z^{\mathrm{cyl}}(\tau) &= 1 + \frac{4}{3\pi\tau} - F\left(-\frac{1}{\tau^2}\right) \\ &= 1 + \frac{4}{3\pi\tau}\left\{1 - \frac{1}{\kappa}[(1-\tau^2)E(\kappa^2) + \tau^2 K(\kappa^2)]\right\}, \end{aligned} \tag{7}$$

where in the first expression we have defined $F(x) \equiv {}_2F_1[-\frac{1}{2}, \frac{1}{2}; 2, x]$, a useful hypergeometric function [24] which will be employed often in the rest of this paper, and the second expression is given in terms of the complete elliptic integrals E and K [24] with $\kappa = 1/\sqrt{1+\tau^2}$. To establish the equivalence of a rotationally symmetric ellipsoid (oblate or prolate as required) to a cylinder with a circular cross section, we first impose the equality between demagnetization factors:

$$N_z(\tau_e) = N_z^{\mathrm{cyl}}(\tau), \tag{8}$$

which determines implicitly a relationship between the two aspect ratios, i.e. $\tau_e = \tau_e(\tau)$. Then, the equal volume condition is imposed:

$$\frac{4}{3}\pi a^2 c = \pi R^2 t \Rightarrow a = R\left(\frac{3}{2}\frac{\tau}{\tau_e}\right)^{1/3}, \tag{9}$$

which determines the correction factor to go with a as soon as the functional dependence of $\tau_e = \tau_e(\tau)$ has been determined from the first condition. The remaining semiaxis, c, is determined by combining the definition of $\tau_e = c/a$ with (9), which results in

$$c = \frac{t}{2}\left(\frac{3}{2}\frac{\tau_e^2}{\tau^2}\right)^{1/3}. \tag{10}$$

Thus, the equivalent ellipsoid is uniquely determined. Figure 1 shows the 'correction factors' to apply in the choice of the equivalent ellipsoid semiaxes. The ratio between the correspondent shape parameters (semiaxis a over disc radius and semiaxis c over half-thickness) can be very different from unity, especially near $\tau = 0$ and for large values of the aspect ratio. Several examples of equivalent ellipsoids for cylinders are shown in figure 1 through a cross-sectional representation

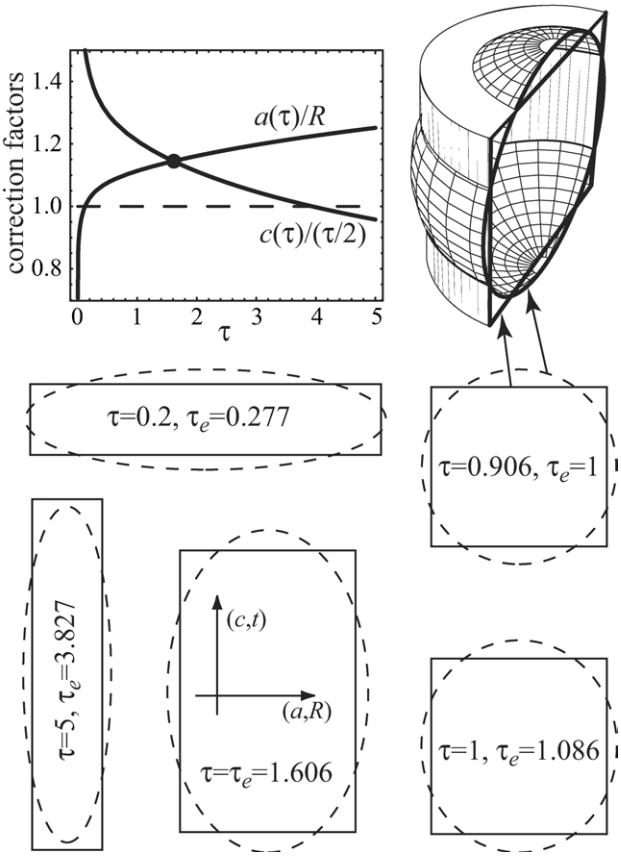

Figure 1. Top left: plot of the 'correction factors' to the ellipsoid semiaxes. Top right: a three-dimensional sketch of the equivalent ellipsoid for a cylinder. Below: examples of equivalent ellipsoids as seen in the axial cross section of the cylinder.

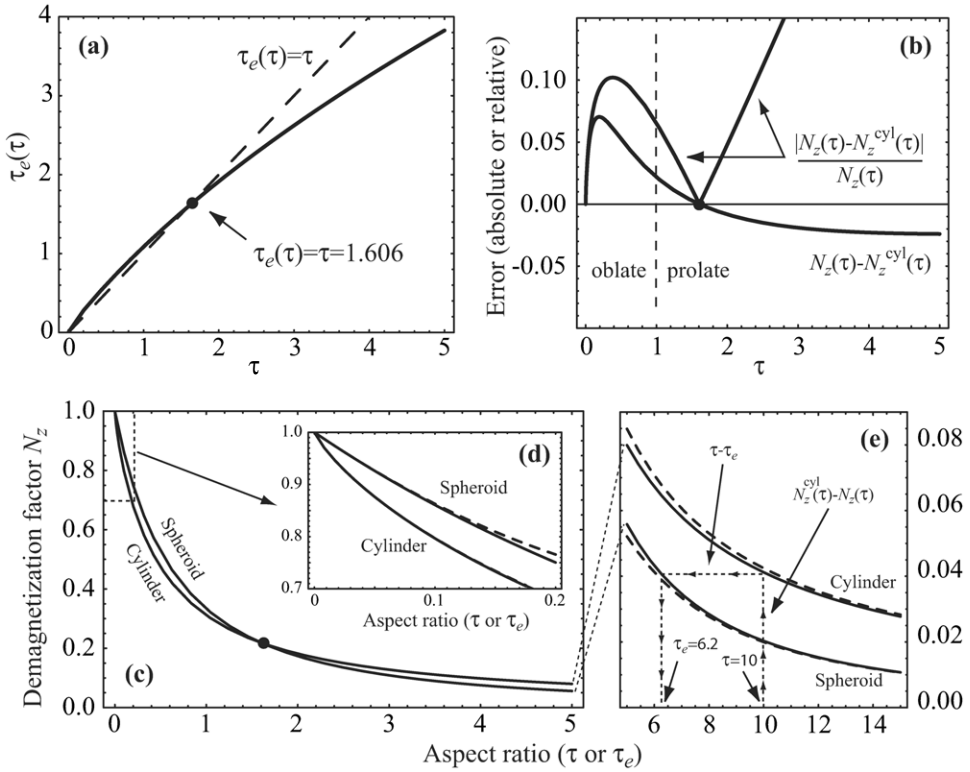

Figure 2. (*a*) The equivalent-ellipsoid aspect ratio, τ_e, as a function of the cylinder aspect ratio, τ. The curve is obtained by numerically solving the equation $N_z(\tau_e) = N_z^{\rm cyl}(\tau)$; (*b*) relative and absolute error, resulting from the choice $\tau_e = \tau$; (*c*) demagnetization factors for cylinders and spheroids (oblate or prolate ellipsoids). The inset (*d*) shows the thin-disc limit $\tau \to 0$, where the dashed lines correspond to expansions in (11). The long cylinder limit $\tau \to \infty$ is shown in (*c*), where the dashed lines correspond to the expansions in (13).

(the meaning of which is clarified in the three-dimensional sketch on the top right) for several values of the cylinder aspect ratio τ. It is worthwhile noting that the cylinder with square cross section ($\tau = 1$) is *not* equivalent to a sphere ($\tau_e = 1$); instead, a sphere is the equivalent ellipsoid of a cylinder with an aspect ratio of $\tau = 0.906$. We might also note that, consistent with the trend of the 'correction factors', when the aspect ratio of the cylinder becomes larger than 3.9, a value obtained by imposing $c = t/2$ in (10), the equivalent (prolate) spheroid long axis, c, is always smaller than the cylinder height $t/2$ (i.e. the top and bottom parts of the oval cross section do not touch the cylinder upper and lower surfaces). An example is shown at the bottom left, for $\tau = 5$. Similarly, for very thin discs with an aspect ratio below 0.12, obtained by imposing $a = R$ in (9), the equivalent (oblate) spheroid equatorial circle is always inscribed in the cylinder circular cross section.

Examining figure 2(*a*), where the function $\tau_e(\tau)$ is plotted, one can observe that the 'commonsense' choice $\tau_e = \tau$ (represented by the dashed line in figure 2(*a*)) in determining the equivalent ellipsoid is almost never acceptable. The two curves only intersect for $\tau = 0$ (infinitely thin disc) and for $\tau = 1.606$. For any other value of the cylinder aspect ratio, the by-hand imposition of equal aspect ratios introduces errors in the demagnetization factor of the equivalent ellipsoid and, therefore, in the associated magnetostatic energy. This is clearly exhibited in figure 2(*b*), where the difference between the demagnetization factors for the cylinder and for the ellipsoid with the 'commonsense' choice $\tau_e = \tau$ is plotted in absolute and relative terms. It can be noticed that, while the error in absolute terms always remains below 0.07, the relative error can be arbitrarily high. For thin discs versus oblate spheroids (the region $\tau < 1$), the relative error reaches a maximum of about 10% at $\tau = 0.38$. Considering rods versus prolate spheroids, $\tau > 1$, the approximation becomes worse with the relative error increasing linearly with the aspect ratio. Therefore, when equivalent-ellipsoid estimates are used for rods, particular care is needed in order to ensure sufficient accuracy.

It is instructive to consider the asymptotic behaviour of the demagnetization factors for very thin ($\tau \to 0$) or very long ($\tau \to \infty$) cylinders. In both cases, one can establish a more direct connection between a thin or thick cylinder and its equivalent ellipsoid, as the function $\tau_e(\tau)$ can be given explicitly. When $\tau \to 0$, one can expand the two demagnetization factors as follows:

$$N_z(\tau_e) = 1 - \frac{\pi}{2}\tau_e + 2\tau_e^2 + O(\tau_e^3),$$
$$N_z^{\rm cyl}(\tau) = 1 + \frac{\tau}{\pi}\left(1 + \log\frac{\tau^2}{16}\right) + O(\tau^3). \qquad (11)$$

The two functions $N_z(\tau_e)$ and $N_z^{\rm cyl}(\tau)$ are plotted in figure 2(*c*) in the range ($0 < \tau < 5$), together with their expansions for $\tau \to 0$, shown in figure 2(*d*). The inset (*d*) reveals the accuracy of the approximated expression for cylinders: only one dashed line, for spheroids, is visible, as the curve for cylinder coincides with the correct expression (continuous line) at least in the restricted range ($0 < \tau < 0.2$).

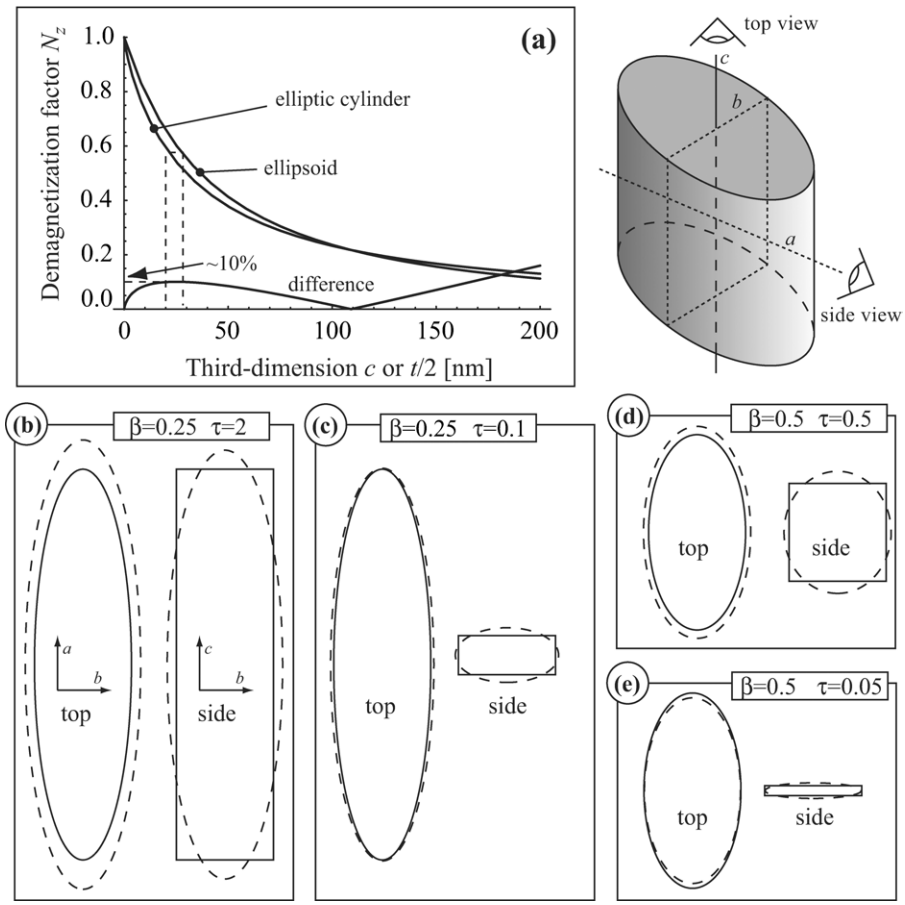

Figure 3. (*a*) Comparison between the demagnetization factor of an ellipsoid and an elliptic cylinder with identical lateral semiaxes $a = a' = 100\,\text{nm}$, $b = b' = 50\,\text{nm}$ and a variable third dimension c or $t/2$. At the bottom of (*a*), the relative difference between the demagnetization factors. On the right, a three-dimensional sketch of the two perspectives used to draw the figures below. (*b*)–(*e*) Four examples of equivalent ellipsoids for elliptic cylinders (top and side views given for each case, as sketched above).

The equality between the demagnetization factors results in this limit in the following solution for the equivalent ellipsoid aspect ratio

$$\tau_e = \frac{\pi}{8}\left[1 - \sqrt{1 + \frac{32\tau}{\pi^3}\left(1 + \log\frac{\tau^2}{16}\right)}\right], \qquad (12)$$

which, evidently, is rather different from the 'commonsense' choice $\tau_e = \tau$.

The asymptotic behaviour of the demagnetization factor for long cylinders ($\tau \to \infty$) is as follows:

$$N_z(\tau_e) = \frac{\log(2\tau_e) - 1}{\tau_e^2} + O(\tau_e^{-4}),$$
$$N_z^{\text{cyl}}(\tau) = \frac{4}{3\pi\tau} - \frac{8}{\tau^2} + O(\tau^{-4}). \qquad (13)$$

The curves corresponding to these expansions are plotted as dashed lines in figure 2(*e*) within the range ($5 < \tau < 15$), together with the correct expressions (continuous lines). Equation (13) shows explicitly how the difference between τ_e and τ becomes increasingly larger: the leading terms in the two demagnetization factors are different, being τ_e^{-2} and τ^{-1}, respectively. Consequently, the equality between demagnetization factors results in a quasi-linear divergence of the quantity, $\tau - \tau_e$. In other words, the difference in aspect ratios between the long cylinder and its equivalent ellipsoid can be arbitrarily large. For instance, a cylinder with an aspect ratio of $\tau = 10$ has an equivalent ellipsoid of the aspect ratio, $\tau_e = 6.2$, as shown in figure 2(*e*), while for $\tau = 100$ we have $\tau_e = 26.5$, almost four times less. Again, and clearly, the intuitive criterion $\tau_e = \tau$ simply fails by a long shot.

4. The equivalent ellipsoid for cylinders with elliptical cross section

Let us now investigate the difference between the N_z demagnetization factors for an elliptic cylinder of semiaxes $a' = 100\,\text{nm}$, $b' = 50\,\text{nm}$ and a variable thickness t and for an ellipsoid of semiaxes (a, b, c). Suppose we want to employ another intuitive criterion for finding the equivalent ellipsoid, which would be for instance setting $a = a', b = b'$ (equal cross section) and adjusting c in order to have the same N_z. The two demagnetization factors as functions of the third dimension (c or $t/2$) are shown in figure 3(*a*). The difference between the two curves, which reaches a maximum of 10% around 25 nm, is also displayed. It is clear from the plot that no easy criterion can be established for the relationship between c and t. For instance, if we have $t/2 = 20\,\text{nm}$ then $N_z^{\text{e.c.}} = 0.59$, which implies (following the dashed line) $c = 26\,\text{nm}$. However, in

order to have equal volume, we would need $c = 3t/4 = 30\,\mathrm{nm}$, which is not consistent with the equality of the N_z factors. As a result of the application of some intuitively plausible, handy criterion in finding the equivalent ellipsoid, in this case choosing $a = a'$ and $b = b'$, we invariably introduce some error in the magnetostatic energy.

To determine the correct equivalent ellipsoid for an elliptic cylinder, we begin by imposing the equal volume condition:

$$\frac{4\pi}{3}abc = \pi a' b' t. \tag{14}$$

Introducing the dimensionless parameters $\beta \equiv b'/a'$ and $\tau \equiv t/2a'$, we can solve this relation for the semiaxes of the ellipsoid:

$$\begin{aligned} a &= a' \left(\frac{3}{2}\frac{\beta\tau\tau_b}{\tau_a^2}\right)^{1/3}, \\ b &= b' \left(\frac{3}{2}\frac{\tau\tau_a}{\beta^2\tau_b^2}\right)^{1/3}, \\ c &= \frac{t}{2} \left(\frac{3}{2}\frac{\beta\tau_a\tau_b}{\tau^2}\right)^{1/3}, \end{aligned} \tag{15}$$

where the equivalent ellipsoid aspect ratios, τ_a and τ_b, are determined from the following two conditions on the demagnetization factors:

$$N_z\left(\frac{1}{\tau_a}, \frac{\tau_b}{\tau_a}\right) = N_x^{\mathrm{e.c.}}(\beta, \tau), \tag{16}$$

$$N_z(\tau_a, \tau_b) = N_z^{\mathrm{e.c.}}(\beta, \tau). \tag{17}$$

For a given elliptic cylinder shape (β, τ), these equations can be solved numerically for (τ_a, τ_b), and then the equivalent ellipsoid semiaxes are determined from (15). A practical example is shown in appendix A, where the ellipsoid equivalent to an elliptic cylinder with $\beta = 1/2$ and $\tau = 1/2$ is determined exactly.

The expressions for the demagnetization factors of the elliptic cylinder suitable for numerical integration are [25]

$$\begin{aligned} N_z^{\mathrm{e.c.}}(\beta, \tau) &= 1 + \frac{8\beta}{3\pi^2\tau} K(1-\beta^2) \\ &\quad - \frac{2}{\pi}\int_0^{\pi/2} \mathrm{d}\phi\, F\left[-\frac{\beta^2}{\tau^2 g(\beta,\phi)}\right], \end{aligned} \tag{18}$$

$$\begin{aligned} N_x^{\mathrm{e.c.}}(\beta, \tau) &= \frac{8\beta}{3\pi^2\tau(1-\beta^2)}[\beta^2 K(1-\beta^2) - E(1-\beta^2)] \\ &\quad + \frac{2\beta^2}{\pi}\int_0^{\pi/2} \mathrm{d}\phi \frac{\cos^2\phi}{g(\beta,\phi)} F\left[-\frac{\beta^2}{\tau^2 g(\beta,\phi)}\right], \end{aligned} \tag{19}$$

where $g(\beta, \phi) \equiv 1 - (1-\beta^2)\cos^2\phi = \sin^2\phi + \beta^2\cos^2\phi$ and F is the hypergeometric function, introduced right after (7). Examples of exact equivalent ellipsoids for elliptic cylinders of various shape parameters are given in figure 3 by displaying two perpendicular cross sections, the top view and the side view, as clarified better in the top right part of the figure. Consistent with the trend of the error plot in (*a*) and with the results obtained for circular cylinders, the largest deviations from the 'commonsense' choice, which in this case is in the guise of the approximations $\tau_a/\tau_b = b/a \sim \beta$ and $\tau_a \sim \tau$, are observed for large values of τ, i.e. for elliptic rods (cf the example on the bottom left of figure 3).

5. The equivalent ellipsoid for rectangular prisms

The demagnetization factors for the prism with edge lengths $(2L_x, 2L_y, 2L_z)$ and volume $V = 8L_xL_yL_z$ can be computed using the magnetometric tensor-field formalism introduced in [26]. The demagnetization factors are given by

$$\begin{aligned} N_\alpha^p &= \frac{1}{\pi^3 V}\int_0^{2L_x}\mathrm{d}x\int_0^{2L_y}\mathrm{d}y\int_0^{2L_z}\mathrm{d}z(2L_x - x)(2L_y - y) \\ &\quad \times(2L_z - z)\mathcal{D}^{\alpha\alpha}(\boldsymbol{r}), \end{aligned} \tag{20}$$

where $\mathcal{D}^{\alpha\beta}(\boldsymbol{r}) = 1/4\pi r^5[r^2\delta^{\alpha\beta} - 3r^\alpha r^\beta]$ is the dipolar tensor. We introduce the dimensionless aspect ratios: $\lambda_y \equiv L_y/L_x$ and $\lambda_z \equiv L_z/L_x$. The integrations are elementary and the result for N_z^p is

$$\begin{aligned} N_z^p = G(\lambda_y, \lambda_z) \equiv \frac{1}{3\pi\lambda_y\lambda_z}\Bigg\{ &-2 + \lambda_y^3 + \lambda_z^3 + (2-\lambda_y^2)\bar{\lambda}_y \\ &+(2-\lambda_z^2)\bar{\lambda}_z - \bar{\lambda}_{yz}^3 + (-2+\lambda_y^2+\lambda_z^2)\Lambda - 3\lambda_y\ln(\lambda_y + \bar{\lambda}_y) \\ &-3\lambda_z\ln(\lambda_z + \bar{\lambda}_z) + 6\lambda_y\lambda_z\arctan\left(\frac{\lambda_y\lambda_z}{\Lambda}\right) \\ &-3\lambda_y\lambda_z\ln(\lambda_y^{\lambda_y}\lambda_z^{\lambda_z}) + 3\lambda_y(\lambda_z^2 - 1)\ln\left(\frac{\bar{\lambda}_z}{\lambda_y + \Lambda}\right) \\ &+3\lambda_z(\lambda_y^2 - 1)\ln\left(\frac{\bar{\lambda}_y}{\lambda_z + \Lambda}\right) + 3\lambda_y\lambda_z^2\ln(\lambda_y + \bar{\lambda}_{yz}) \\ &+3\lambda_y^2\lambda_z\ln(\lambda_z + \bar{\lambda}_{yz})\Bigg\}, \end{aligned} \tag{21}$$

where $\bar{\lambda}_y \equiv \sqrt{1+\lambda_y^2}$, $\bar{\lambda}_z \equiv \sqrt{1+\lambda_z^2}$, $\bar{\lambda}_{yz} \equiv \sqrt{\lambda_y^2+\lambda_z^2}$ and $\Lambda \equiv \sqrt{1+\lambda_y^2+\lambda_z^2}$. The expression in (21) is equivalent to those reported in the literature [3, 14, 15].

Using the same symmetry argument as for the ellipsoids, the remaining two demagnetization factors can be derived from the above expression by cyclic permutation of the arguments:

$$\begin{aligned} N_x^p(L_x, L_y, L_z) &= G(\lambda_y, \lambda_z), \\ N_y^p(L_x, L_y, L_z) &= G\left(\frac{\lambda_z}{\lambda_y}, \frac{1}{\lambda_y}\right), \\ N_z^p(L_x, L_y, L_z) &= G\left(\frac{1}{\lambda_z}, \frac{\lambda_y}{\lambda_z}\right). \end{aligned} \tag{22}$$

We can use these expressions to determine the equivalent ellipsoid for the rectangular prism. The equal-volume relation is given by

$$\frac{4\pi}{3}abc = 8L_xL_yL_z. \tag{23}$$

Equating the x and y demagnetization factors for the prism to the corresponding factors for the triaxial ellipsoid results in two equations with two unknowns, from which τ_a and τ_b can be determined for a given pair (λ_y, λ_z):

$$\begin{aligned} N_z\left(\frac{1}{\tau_a}, \frac{\tau_b}{\tau_a}\right) &= G(\lambda_y, \lambda_z), \\ N_z\left(\frac{\tau_a}{\tau_b}, \frac{1}{\tau_b}\right) &= G\left(\frac{\lambda_z}{\lambda_y}, \frac{1}{\lambda_y}\right). \end{aligned} \tag{24}$$

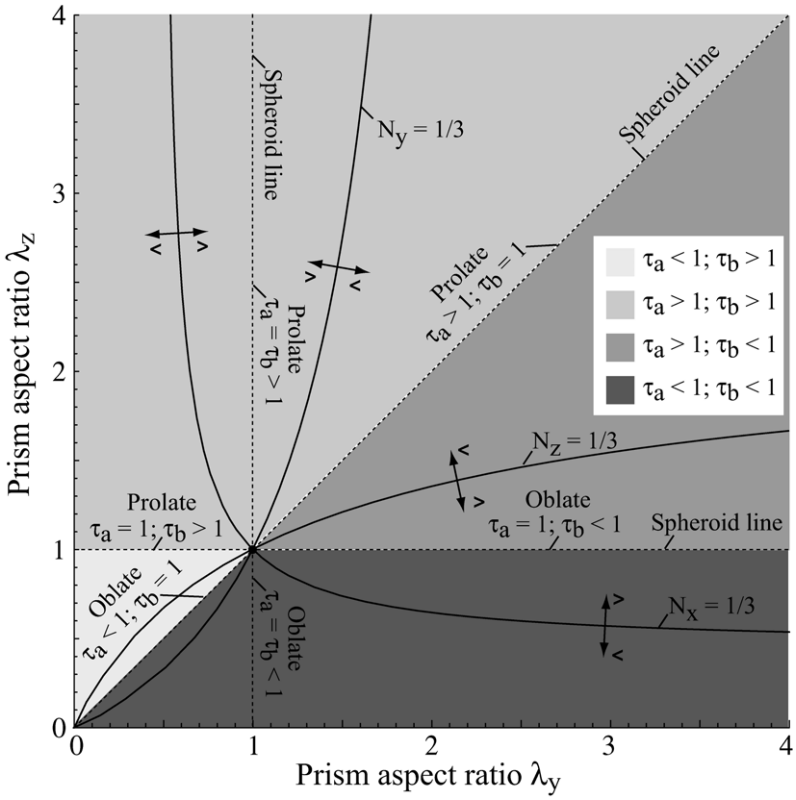

Figure 4. Schematic representation of the equivalent ellipsoid for a rectangular prism as a function of its aspect ratios, λ_y and λ_z.

The results for the equivalent ellipsoid semiaxes (a, b, c) are then

$$a = L_x \left(\frac{6\lambda_y \lambda_z \tau_b}{\pi \tau_a^2} \right)^{1/3},$$
$$b = L_y \left(\frac{6\lambda_z \tau_a}{\pi \lambda_y^2 \tau_b^2} \right)^{1/3}, \qquad (25)$$
$$c = L_z \left(\frac{6\tau_a \tau_b \lambda_y}{\pi \lambda_z^2} \right)^{1/3}.$$

It is instructive to create a diagram showing the equivalent-ellipsoid aspect ratios as a function of the prism aspect ratios, λ_y and λ_z. Such a diagram is shown in figure 4. The solid curved lines represent the loci of points where one of the demagnetization factors is equal to one-third, i.e. $N_i(\lambda_y, \lambda_z) = \frac{1}{3}$. They intersect at the point (1, 1), where the equivalent ellipsoid is a sphere. For each curved line, a double-headed arrow indicates in which direction the demagnetization factor becomes greater (>) or less (<) than one-third. The dashed straight lines represent the loci of points where the equivalent ellipsoid is a spheroid, i.e. two of its semiaxes are of equal length, with oblate and prolate regions as indicated. There are three such lines, corresponding to the cases $a = b \neq c$, $a = c \neq b$ and $b = c \neq a$. On the one side of the point of highest symmetry (the sphere) (1, 1), the straight line corresponds to an oblate spheroid; on the other side, it corresponds to a prolate spheroid. Altogether, there are four shaded areas in the diagram. They cover the four possible cases for the equivalent-ellipsoid aspect ratios: (i) $\tau_a < 1$, $\tau_b < 1$; (ii) $\tau_a < 1$, $\tau_b > 1$; (iii) $\tau_a > 1$, $\tau_b < 1$ and (iv) $\tau_a > 1$, $\tau_b > 1$. The equivalent ellipsoid is a sphere at the point of highest symmetry where all the curves and spheroid lines intersect.

In an alternative and more quantitative representation, we plot the isolines of constant $\tau_a(\lambda_y, \lambda_z)$ and $\tau_b(\lambda_y, \lambda_z)$ in figure 5. The lines were calculated numerically from equation (24) by computing τ_a and τ_b on a square grid of λ_y, λ_z values and then superimposing contours of constant τ_a and τ_b onto the grid. In this way, one can read directly from the drawing the aspect ratios of the equivalent ellipsoid for any prism aspect ratios within the range 0.1–4.0. The plot can be easily extended to cover any range of aspect ratios that might be of interest. The *Mathematica* [27] code used to generate this plot is reported in appendix A. The equivalent ellipsoid aspect ratios can then be used to calculate its semiaxes values by means of (25).

6. Conclusions

While it is true that the energetics of a uniformly magnetized body can be described as if the body were an ellipsoid, we believe to have demonstrated that it is not a trivial problem to establish *which* ellipsoid is actually equivalent to a given shape. We have systematically developed a transparent and easy-to-implement scheme for magnetostatic mapping of complicated shapes onto the ellipsoid. In particular, the mapping has been introduced on the example of the circular cylinder. The elliptic cylinder and the general rectangular prism have then been mapped onto their magnetostatic ellipsoidal counterpart in a most general fashion. In each case, the mapping has been

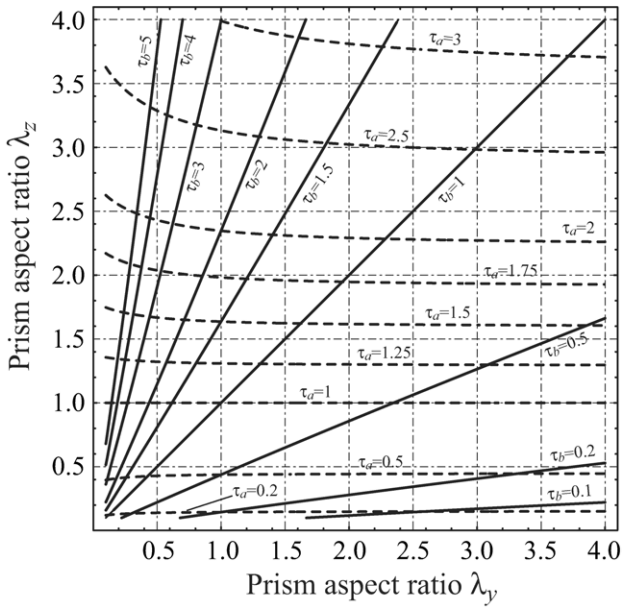

Figure 5. Relation between the equivalent ellipsoid aspect ratios (τ_a, τ_b) and the prism aspect ratios (λ_y, λ_z). The solid lines are for constant τ_b, whereas the dashed lines have constant τ_a.

uniquely defined by the requirement of the two shapes having equal volume and equal magnetostatic energetics (hence, equal demagnetization factors). It is only natural to use the same criteria for any arbitrary shape.

In all the cases considered, the equivalent ellipsoid has been completely specified through the establishment of explicit relationships linking the ellipsoid axes with the shape parameters of the nonellipsoidal bodies. As an important corollary of this specification, one is now in a position to determine the errors involved in the naive assumption that equal aspect ratios imply equal demagnetization factors. Thus, while this 'commonsense' assumption is likely to remain the first guess in practical considerations, one is no longer bound to stay with this crude approximation. The method itself, being quite flexible, is much more important than the particular results for the examined shapes. It can be applied to more sophisticated, yet practically significant, cases. One such class comprises multiply connected shapes such as rings and toroids. Another application is to the equivalence of bodies made of different ferromagnetic material. Work along these lines is under way.

It cannot be sufficiently emphasized that the very examination of the magnetostatic equivalence of untrivial shapes, such as those depending on two dimensionless parameters, has only been possible because of the very recent breakthrough in the exact determination of the demagnetization factors of arbitrary bodies by means of the Fourier-space technique [5, 6, 19].

Acknowledgments

Stimulating discussions with S Tandon and Y Zhu and financial support by the US Department of Energy (Basic Energy Sciences) under contract numbers DE-FG02-01ER45893 and DE-AC02-98CH10886 are gratefully acknowledged by two of us (MB and MDG).

Appendix A

All the figures in this paper were generated using *Mathematica* [27]. We report the essential parts of the code we developed in order to facilitate the interested reader with the practical determination of equivalent ellipsoids for bodies/particles of various shape. Complete *Mathematica* notebooks are available upon request from the corresponding author (MB).

Appendix A.1. Demagnetization factors for bodies of different shape

Cylinder

```
NzCyl[τ_]=1+4/(3 Pi τ)
 -Hypergeometric2F1[-1/2,1/2,2,-1/τ^2];
```

Elliptic cylinder

```
NzEllCyl[β_,τ_] := 1+8β/(3 Pi^2 τ)
 EllipticK[1-β^2]- 2/Pi NIntegrate
  [Hypergeometric2F1[-1/2,1/2,2,-β^2/
   (τ^2(1-(1-β^2) Cos[ϕ]^2))],{ϕ, 0, Pi/2}]
NxEllCyl[β_,τ_] := 8β/(3 Pi^2 τ (1-β^2))
 (β^2 EllipticK[1-β^2]-EllipticE[1-β^2])
  +2β^2/Pi NIntegrate[Cos[ϕ]^2/(1-(1-β^2)
   Cos [ϕ]^2)Hypergeometric2F1[-1/2,1/2,2,
    -β^2/(τ^2(1-(1-β^2) Cos[ϕ]^2))],
     {ϕ, 0, Pi/2}]
```

Prism

$$
\begin{aligned}
\texttt{G[}\lambda y\_,\lambda z\_\texttt{]} = \frac{1}{3\pi\,\lambda y\,\lambda z}\Bigg(& (-2+\lambda y^3+\lambda z^3)+(2-\lambda y^2)\sqrt{1+\lambda y^2}+(2-\lambda z^2)\sqrt{1+\lambda z^2}-(\lambda y^2+\lambda z^2)^{3/2} \\
& +(-2+\lambda y^2+\lambda z^2)\sqrt{1+\lambda y^2+\lambda z^2} \\
& +6\lambda y\,\lambda z\,\texttt{ArcTan}\left[\frac{\lambda y\,\lambda z}{\sqrt{1+\lambda y^2+\lambda z^2}}\right] \\
& -3\lambda y\,\texttt{Log}\left[\lambda y+\sqrt{1+\lambda y^2}\right]-3\lambda z\,\texttt{Log}\left[\lambda z+\sqrt{1+\lambda z^2}\right] \\
& -3\lambda y\,\lambda z\,\texttt{Log}[\lambda z^{\lambda z}\,\lambda y^{\lambda y}] \\
& +3\lambda y(\lambda z^2-1)\,\texttt{Log}\left[\frac{\sqrt{1+\lambda z^2}}{\lambda y+\sqrt{1+\lambda y^2+\lambda z^2}}\right] \\
& +3(\lambda y^2-1)\lambda z\,\texttt{Log}\left[\frac{\sqrt{1+\lambda y^2}}{\lambda z+\sqrt{1+\lambda y^2+\lambda z^2}}\right] \\
& +3\lambda y\,\lambda z^2\,\texttt{Log}\left[\lambda y+\sqrt{\lambda y^2+\lambda z^2}\right] \\
& +3\lambda y^2\,\lambda z\,\texttt{Log}\left[\lambda z+\sqrt{\lambda y^2+\lambda z^2}\right]\Bigg);
\end{aligned}
$$

```
NxPri[λy_,λz_] = G[λy,λz];
NyPri[λy_,λz_] = G[λz/λy,1/λy];
NzPri[λy_,λz_] = G[1/λz,λy/λz];
```

Spheroid

```
NzSph[τe_] = 1/(1-τe^2)(1-τe ArcCos[τe]/
  Sqrt[1-τe^2]);
```

Ellipsoid

```
NzEll[τa_,τb_] = Re[τb/(τb^2-1) 1/Sqrt[τa^2-1]
  (EllipticF[ArcSin[Sqrt[1-τa^(-2)]],
  (1-τb^(-2))/(1-τa^(-2))]
  -EllipticE[ArcSin[Sqrt[1-τa^(-2)]],
  (1-τb^(-2))/(1-τa^(-2))])];
NzEll[τa_,τa_]=NzSph[τa];
NxEll[τa_,τb_]=NzEll[1/τa,τb/τa];
NyEll[τa_,τb_]=NzEll[τa/τb,1/τb];
```

Appendix A.2. Determination of the equivalent ellipsoids for some representative cases

Appendix A.2.1. The equivalent spheroid for a cylinder (the procedure is essentially the same for all other cases where the shape is specified by a single dimensionless ratio)

```
tauEquiv[τ_]:= FindRoot[NzCyl[τ] == NzSph[τe],
   {τe,1/2τ,3/2τ}][[1,2]].
```

In this example, the cylinder has $\tau = 0.2$; it is shown in figure 1.

```
τval=0.2;
τesol=tauEquiv[τval]

{aEll→R(3/2τval/τesol)^(1/3),
  cEll→t2Cyl(3/2τesol^2/τval^2)^(1/3)}.
```

Appendix A.2.2. The equivalent ellipsoids for an elliptic cylinder (the procedure is essentially the same for all other cases where the shape is specified by two dimensionless ratios)

In this example, the elliptic cylinder has $\beta = 1/2$, $\tau = 1/2$; it is shown in figure 3(*d*).

```
βval=1/2;
τval=1/2;

eqEllSol=FindRoot[
  {NzEllCyl[βval,τval]==NzEll[τa,τb],
  NxEllCyl [βval,τval]==NzEll[1/τa,τb/τa]},
  {τa,1/2τval,3/2τval},
  {τb,1/2τval/βval,3/2τval/βval}]

{aEll→aCyl(3/2βval τval τb/
   τa^2)^(1/3)/.eqEll1Sol,
   bEll→bCyl(3/2τval τa/
   (βval^2 τb^2))^(1/3)/.eqEllSol,
   cEll→t2Cyl(3/2βval τa τb/
   τval^2)^(1/3)/.eqEllSol}
```

Appendix A.2.3. Graphical presentation of the equivalent ellipsoids for prisms (figure 5)

```
tauAequiv[λy_,λz_] :=
   FindRoot[{NzEll[1/τa,τb/τa] == G[λy,λz],
   Nz[τa/τb,1/τb]==G[λz/λy,1/λy]},
   {τa,1/2λz,3/2λz},{τb,1/2λz/λy,3/2λz/λy},
   MaxIterations→300][[1,2]]

tauBequiv[λy_,λz_] :=
   FindRoot[{NzEll[1/τa,τb/τa] == G[λy,λz],
   Nz[τa/τb,1/τb]==G[λz/λy,1/λy]},
   {τa,1/2λz,3/2λz},{τb,1/2λz/λy,3/2λz/λy},
   MaxIterations→300][[2,2]]
```

```
contA = {0.2, 0.5, 1.0, 1.25, 1.5, 1.75, 2.0, 2.5, 3.0};
contB = {0.1, 0.2, 0.5, 1.0, 1.5, 2.0, 3.0, 4.0, 5.0};

plA=ContourPlot[tauAequiv[λy,λz],
   {λy,0.1,4},{λz,0.1,4},ContourShading→False,
   PlotPoints→128,Contours→contA,
   PlotRange→All, DisplayFunction→Identity];

plB=ContourPlot[tauBequiv[λy,λz],
   {λy,0.1,4},{λz,0.1,4},ContourShading→False,
   PlotPoints→128,Contours→contB,
   PlotRange→All,DisplayFunction→Identity];

Show[plA,plB,DisplayFunction→
   $DisplayFunction];
```

References

[1] Brown W F and Morrish A H 1957 *Phys. Rev.* **105** 1198
[2] Brown W F 1960 *Am. J. Phys.* **28** 542
[3] Rowlands G 1956 Magnetising energies and domain structures in ferromagnetics *PhD Thesis* University of Leeds
[4] Millev Y T, Vedmedenko E and Oepen H P 2003 *J. Phys. D: Appl. Phys.* **36** 2945
[5] Beleggia M and De Graef M 2003 *J. Magn. Magn. Mater.* **263** L1
[6] Tandon S, Beleggia M, Zhu Y and De Graef M 2004 *J. Magn. Magn. Mater.* **271** 9
[7] Rhodes P, Rowlands G and Birchall D R 1956 *J. Phys. Soc. Japan* **17** 543
[8] Joseph R I 1966 *J. Appl. Phys.* **37** 4639
[9] Chen D-X, Brug J A and Goldfarb R B 1991 *IEEE Trans. Magn.* **27** 3601
[10] Brown W F Jr 1962 *Magnetostatic Principles in Ferromagnetism* (Amsterdam: North-Holland)
[11] Osborn J A 1945 *Phys. Rev.* **67** 351
[12] Stoner E C 1945 *Phil. Mag.* **36** 803
[13] Vedmedenko E Y, Oepen H P and Kirschner J 2003 *J. Magn. Magn. Mater.* **256** 237
[14] Rhodes P and Rowlands G 1954 *Proc. Leeds Phil. Soc.* **6** 191
[15] Aharoni A 1998 *J. Appl. Phys.* **83** 3432
[16] Chen D-X, Pardo E and Sanchez A 2002 *IEEE Trans. Magn.* **38** 1742
[17] Chen D-X 2001 *J. Appl. Phys.* **89** 3413
[18] Millev Y T 2002 *Bull. APS* **47** 21
[19] Tandon S, Beleggia M, Zhu Y and De Graef M 2004 *J. Magn. Magn. Mater.* **271** 27
[20] Aharoni A 1996 *Ferromagnetism* (Oxford: Oxford University Press)
[21] Hubert A and Schäfer R 1998 *Magnetic Domains* (Berlin: Springer)
[22] Moskowitz R and Della Torre E 1966 *IEEE Trans. Magn.* **2** 739
[23] Landau L D and Lifshitz E M 1960 *Course of Theoretical Physics: Electrodynamics of Continuous Media* vol 8 (Oxford: Pergamon)
[24] Abramowitz M and Stegun I 1972 *Handbook of Mathematical Functions* (New York: Dover)
[25] Beleggia M, De Graef M, Millev Y, Goode D A and Rowlands G 2005 *J. Phys. D: Appl. Phys.* **38** 3333
[26] Beleggia M and De Graef M 2005 *J. Magn. Magn. Mater.* **285** L1
[27] Wolfram S 1999 *Mathematica* (Wolfram Research Inc., Champaign, IL) Version 4.0.